January 2014

Stress And Rest Spect/ct Imaging For Evaluation Of Lower Extremity Perfusion: An Index For Evaluation Of Microvascular And Macrovascular Disease

Nataly Sumarriva

Stress and Rest SPECT/CT Imaging for Evaluation of Lower Extremity

Perfusion: An Index for Evaluation of Microvascular and Macrovascular Disease

A Thesis Submitted to the

Yale University School of Medicine

in Partial Fulfillment of the Requirements for the

Degree of Doctor of Medicine

By

Nataly Sumarriva

2014

Abstract

STRESS AND REST SPECT/CT IMAGING FOR EVALUATION OF LOWER EXTREMITY

PERFUSION. Nataly Sumarriva, Wunan Zhou, Mitchel R. Stacy, and Albert J. Sinusas. Section of

Cardiology, Department of Internal Medicine, Yale University, School of Medicine, New Haven,

CT.

Peripheral arterial disease (PAD) is a progressive atherosclerotic disease of the lower limbs

affecting approximately 8 to 10 million Americans. Diabetic patients are twice as likely to

develop PAD than are patients without diabetes mellitus (DM) and PAD progression is more rapid

in DM patients. The primary goal of this study was to translate image analysis tools previously

developed and validated for application to hybrid SPECT/CT imaging in preclinical models of

peripheral arterial disease to patients, and to evaluate the reproducibility and feasibility of the

approach for clinical imaging. Lower extremity tissue perfusion was analyzed in patients using

^{99m}Tc-tetrofosmin SPECT/CT imaging. Image analysis tools previously validated for murine and

porcine models of hind limb ischemia were used to analyze and quantify specific lower extremity

muscle groups in a pilot series of clinical SPECT/CT images. Using an image analysis program,

the image quantification was done by drawing volumes of interest (VOIs) around each of five

muscle groups in the calf (tibialis anterior, tibialis posterior, fibularis, soleus, and gastrocnemius)

on the CT images. These ROIs were then copied onto the registered SPECT images to obtain an

average intensity value for each muscle group an index of both microvascular and macrovascular

perfusion. The results showed a statistically significant difference in intensity per volume per

injected dose of radiotracer corrected for decay between rest and stress for all of the muscle groups

between patients that had both rest and stress imaging (P=0.001). We demonstrated that our

approach has a high interobserver reproducibility, with an R^2 = 0.99 between the two sets of

values. This method may be used to assess abnormality of both microvascular and macrovascular

perfusion of patients with diabetes mellitus at higher risk for peripheral arterial disease in the

future.

Acknowledgements

I would like to thank first and foremost my advisor on this project, Albert J. Sinusas, MD, for allowing me the great opportunity to work on a project that I am truly interested in and for teaching me how to think like a researcher. I would also like to thank the many others in the Sinusas lab. These include Mitchel Stacy, PhD, who has provided me with much guidance and generous help throughout this project, Wunan Zhou, MD, for her great ideas and help, especially in the times that help was most needed on this project, and Stephanie Thorn, PhD, who contributed ideas that went into this thesis. I would also like to thank my academic advisor, Patrick O'Connor, MD, and our Dean of Student Affairs, Nancy Angoff, MD, for their continuous support and encouragement. I would like to thank also my close friends John Ramirez, MD, Alex Marzuka, MD, Catherine Yang, MD, Oluwatosin Onibokun, MD, and Sarah El-Ghazaly, JD, for their faith in me. Sincere gratitude also goes to Thomas Beck, PhD, who offered much generous support and help during the writing of this thesis. I cannot say a note of thanks without including the most incredible and influential people in my life – my mother Elsa, father Edmundo, brother Gonzalo, and sister Katherine. Much gratitude goes to the YSM Office of Student Research for their generous funding to help with this project. Thank you to the Yale School of Medicine for granting me the wonderful opportunity, skills, and knowledge to heal others through the art of medicine. Finally, none of this would have been possible for me to accomplish without God, for every event that has occurred, every encounter that has been made, and every lesson that has been learned, has been according to His will.

Table of Contents

Introduction

Peripheral Arterial Disease (PAD)

Peripheral arterial disease (PAD) is a progressive atherosclerotic disease of non-cerebral and non-coronary arteries affecting approximately 8 to 10 million Americans.[1] The development of PAD is multifactorial and depends on both modifiable and non-modifiable factors, such as age, sex, ethnicity, smoking habits, and the presence of co-morbidities such as diabetes mellitus (DM), hypertension (HTN), and hyperlipidemia (HLD), and is also associated with chronic renal insufficiency. Patients who develop PAD can be asymptomatic, and those that do develop symptoms most often present with intermittent claudication. Because PAD most often affects the superficial femoral artery, which is located in the thigh, pain is usually felt distally in the calf.[1]

Detection and Evaluation of PAD

Various methods exist for evaluating perfusion and diagnosing vascular disease in clinical practice. These include the ankle-brachial index (ABI), toe-brachial index (TBI), duplex ultrasound, segmental blood pressures, transcutaneous oxygen assessment, magnetic resonance imaging (MRI), and computed tomography (CT) angiography. Each of these imaging approaches has strengths and weaknesses.

The ankle-brachial index, which is measured with the aid of a hand-held Doppler machine, is an inexpensive and accessible method of diagnosing PAD in the general population. It is calculated by comparing the blood pressures in the ankles (taken at the dorsalis pedis and posterior tibial arteries) with the blood pressures in the arms. The normal value is between 0.9 and 1.3, and below 0.9 is considered diagnostic for PAD. Above 1.3, it is falsely elevated and is indicative of non-compressibility and likely calcifications. It has a high sensitivity (75%-95%) and specificity (95%-96%) when compared with angiography.[2] When revascularization is being considered, additional imaging may be necessary. In this situation duplex ultrasound is the first-line modality due to the non-invasive nature, as well as high sensitivity (84-87%) and specificity (92-98%) compared to angiography.[1]

Invasive contrast angiography has traditionally served as the gold standard for detection of PAD, although more recently CT angiography and MR angiography have replaced these invasive approaches for evaluating arterial structure in PAD because of their accuracy and non-invasive nature.[1]

Limitations of ABIs

Despite the widespread use of ABIs for diagnosing PAD in clinical practice, there are certain situations in which this method is less reliable for evaluation of PAD. For example, when the ABI value is indeterminate, it is considered falsely elevated, and is indicative of non-compressible arteries with calcifications. This

can be seen in cases of diabetes, chronic kidney disease, or advanced age.[3] Indeed, in a recent study that evaluated patients undergoing both ABI measurements and angiography, Chung et al. showed that the most influential factor affecting the validity of ABI was diabetes, especially when there was concurrent peripheral neuropathy or high risk of arterial medial calcification. In fact, the sensitivity of ABI falls to 53% (specificity 95%) in the presence of peripheral neuropathy.[4] False-normal ABIs (values 0.9 to 1.3) are even more problematic, as calcifications may elevate the pressure in the legs to a normal range, before becoming elevated enough to reach levels deemed indeterminate. Additionally, the ABI is useful for the detection of large but not small vessel or microvascular disease, while it is still possible for muscular ischemia to occur in the absence of large vessel disease.[5]

In cases of indeterminate ABIs, the patient will often be evaluated with the TBI, which is more helpful in detecting microvascular disease, as the blood vessels in the toes are less susceptible to vessel stiffness and calcifications.[6] However, the diagnostic criteria for a pathologic TBI are not well established and there is a lack of evidence-based guidelines. Though several guidelines recommend considering a TBI<0.70 as pathological,[7,8] the current literature is insufficient to conclude a specific cutoff as diagnostic for PAD.[6]

Limitations of Conventional Imaging Approaches

Disadvantages and limitations also exist for the conventional imaging approaches, including duplex ultrasound, MRI, and CT angiography. Drawbacks to duplex ultrasound include its limited penetration depth and inability to assess small vessel or collateral blood flow.[9] MRI has increased spatial resolution and improved tissue penetration, and does allow for imaging of physiological indices like tissue perfusion and oxygenation. However, imaging of tissue of perfusion with MRI often requires evaluation of perfusion during conditions of stress, like exercise, or application of reactive hyperemia protocols with imaging to allow for the detection of pathophysiologic differences in regional tissue perfusion. Furthermore, MR imaging is not ideally suited for targeted molecular imaging. There are fewer targeted MR imaging probes that exist for targeting critical molecular processes associated the development and progression of PAD, compared to nuclear imaging approaches (described below). In addition, MR imaging approaches in general have decreased sensitivity for targeted molecular imaging. CT angiography also offers high resolution and can provide useful anatomical information about the status of the arterial tree, although this approach is not useful for evaluation of vascular reactivity or tissue perfusion in vivo.[9]

Application of Radiotracer-Based Imaging

To identify certain subsets of patients with PAD, one potential specific and sensitive option is single photon emission computed tomography (SPECT) perfusion imaging.[5] The evaluation of perfusion is critical in patients with PAD,

as impaired lower-extremity perfusion is an important pathophysiologic mechanism that drives complications associated with the disease. SPECT perfusion imaging is a valuable tool for evaluation of disease progression and effectiveness of therapy.[10] Previous studies have demonstrated that SPECT imaging is a more sensitive method of detecting PAD in diabetic patients with normal ABIs.[5] Often stress/rest SPECT perfusion is performed in patients with symptomatic PAD who are being considered for surgical revascularization as a means to risk stratify these patients prior to the surgical intervention. Lower extremity SPECT imaging can be performed in conjunction with myocardial SPECT perfusion imaging, without the need for additional radioisotope administration.

To examine lower-extremity skeletal muscle blood flow in patients with vascular disease, the first nuclear medicine studies evaluated the clearance rates of ^{24}Na-chloride, ^{133}Xe, and ^{99m}Tc-pertechnetate after intramuscular injection of these radiotracers. This was followed by the development of 2-dimensional imaging of microspheres and albumin that were radiolabeled with ^{99m}Tc, ^{131}I-sodium, and ^{111}In.[9] However, these 2-dimensional techniques required invasive intra-arterial injections and thus were not ideal. To overcome this limitation, ^{201}Tl was used as a perfusion agent in various studies.[5,11] ^{201}Tl is a tracer with biologic properties similar to potassium. Since it can be transported into viable cells by the sodium-potassium pump, it can serve as a measure of both myocardial and skeletal muscle perfusion. After intravenous injection of this radiotracer, perfusion imaging can

be performed at rest or during exercise. Assessment of PAD severity with perfusion agents, like ^{201}Tl, has traditionally been based on evaluation of ratios of radioactivity between diseased and non-diseased legs, or, in the case of bilateral disease, by normalizing activity in the lower extremities to that of the whole body.[5,11] As 3-dimensional SPECT imaging systems emerged, it became possible to more accurately detect and localize regions of ischemia in the lower extremities under both rest and stress conditions using [201]Tl.

[201]Tl has a long half-life and suboptimal imaging characteristics, resulting in higher radiation exposures and providing a poorer image quality. [201]Tl imaging has largely been replaced by imaging with ^{99m}Tc-labeled perfusion agents which have a shorter half-life, improved imaging characteristics and provide improved imaging quality. These ^{99m}Tc-labeled perfusion agents also show little "redistribution", thus allowing for delayed imaging times after injections during treadmill exercise and measures of peak exercise perfusion at the time of initial injection.[9] For example, in one study by Duet et al., ^{201}Tl scintigraphy was performed both 5 and 30 minutes after exercise to verify that the values remained unchanged during the time necessary to scan the myocardium.[5] However, longer delays in imaging time following a stress injection of ^{201}Tl may result in underestimation of flow heterogeneity induced by stress. This highlights the difficulty in using ^{201}Tl to identify post-exercise blood flow at different time points, due to the redistribution in ischemic tissue. [201]Tl clearance is quite rapid, and its transport across cell membranes is partially mediated by flow.[12] Thus,

clearance rate is slower in ischemic regions with diminished flow, a phenomenon termed "redistribution", which represents differential clearance from normal and ischemic regions. In situations and regions with high flow, such as in the lower extremities during exercise, the clearance of ^{201}Tl is more rapid, and there may appear greater differences in activity depending upon the time from injection of radiotracer to scanning. This problem is not seen when using ^{99m}Tc-labeled perfusion agents like ^{99m}Tc-tetrofosmin, because the clearance of this radiotracer from muscle is much slower. Thus, studies using ^{99m}Tc-labeled perfusion agents may provide a more accurate evaluation of tissue perfusion for later imaging time points following radiotracer injection post-exercise testing.[12]

In addition, an advantage to SPECT imaging is the potential evaluation of multiple radiotracers simultaneously. Although it provides higher sensitivity than CT or MRI, SPECT has lower resolution when compared to these other imaging modalities (millimeter to ~1 cm resolution). With the advent of hybrid SPECT/CT imaging, high-resolution anatomical CT imaging can now be combined with high-sensitivity physiological nuclear imaging to provide more precise radiotracer quantification within specific regions of interest.[9] Furthermore, these hybrid imaging systems allow for attenuation correction, which minimize attenuation artifacts from soft tissue, and for correction of partial-volume effects. This results in more precise radiotracer quantification within anatomically defined regions of interest by CT.[13]

Past Lower Leg Perfusion Imaging Studies

In the study by Duet et al., ^{201}Tl scintigraphy was used to detect lower limb perfusion abnormalities immediately after myocardial perfusion imaging, thus allowing assessment of both coronary and peripheral artery disease. This research group first determined a threshold value of normal peripheral muscular perfusion, i.e., normal post-exercise calf ^{201}Tl muscular uptake, in a control group of nine healthy subjects. For the normal control group, the post-exercise threshold value was set as the mean value of the control group minus 2 SD and was equal to 6%. Afterwards, the accuracy of the threshold value was verified in a pilot group of 25 diabetic patients with previously diagnosed PAD. Finally, the muscular perfusion of a group of 47 asymptomatic diabetic patients with normal or indeterminate ABI readings was assessed through ^{201}Tl scintigraphy.[5] The study concluded that perfusion abnormalities existed in the lower limbs of 38% of the asymptomatic diabetic patients, even though 80% of the patients in this group had ABI values in the normal range and 20% had an inconclusive result.[5] This study highlighted the potential discrepancy between ABIs and perfusion imaging for detection of PAD.

This study also found the perfusion indices of the calves were much higher at 30 minutes post-exercise rather than 4 hours later in the control group, which indicates greater perfusion in the lower extremities at exercise rather than at rest. In the pilot group of 25 patients with proven PAD, post-exercise calf perfusion indices were significantly lower (3.91 +/- 0.83%) than in the control group. Among the 47 diabetic patients in the third group with no symptoms or prior

diagnosis of PAD, 18 patients had a post-exercise ^{201}Tl index that was less than the threshold value of 6%. In this group, perfusion indices did not change significantly between post-exercise and resting time points. This suggests a lack of perfusion reserve during exercise among the diabetic patients.[5]

In another study, Cosson et al.[14] demonstrated skeletal muscle perfusion defects were present in 42% of the diabetic study population. The study investigated 80 diabetic patients with more than one cardiovascular risk factor without claudication, and found that the muscle perfusion defects were mainly in the calves (as compared to the buttocks or thighs) and that these correlated with retinopathy. Furthermore, they demonstrated that in patients with defects in the buttock and/or thigh, there was a higher prevalence of nephropathy and retinopathy than in patients with defects only in the calf. They concluded that proximal defects, as in the thigh or buttock, may thus be due to microvascular disease, while more distal defects may be due to macrovascular disease.

Despite the success of ^{201}Tl studies in detecting changes in perfusion in diabetic and PAD patients, not all studies have shown that this method is useful. One study[15] by Bajnok et al. showed that ^{99m}Tc-sestamibi scintigraphy had false-positive and false-negative results, due to a paradoxically high uptake of the radiotracer in muscles supplied by vessels that were significantly stenosed. In these cases, the post-stress radioactivity in the ischemic muscles was significantly higher than the radioactivity in corresponding regions with no or less ischemia.

This study found a sensitivity of 55% and a specificity of 25% of the scintigraphic method, with an overall accuracy of 50%.

Evaluation of Perfusion to Specific Muscle Groups

Previous studies using SPECT have traditionally evaluated tissue perfusion for the calf by drawing regions of interest around the entire calf, comparing the radioactivity between the affected and unaffected leg, or by normalizing the activity in the calves or lower legs to whole body activity.[9] It may be useful, however, to evaluate tissue perfusion within specific anatomical regions of the lower leg. This more detailed analysis may assist in the translation of image-guided therapies to affectively assess tissue perfusion within specific vascular territories or muscle groups that are most susceptible to complications associated with vascular disease.

Indeed, numerous MRI studies have evaluated the perfusion of individual muscle groups. In these studies, regions of interest were drawn around particular muscle groups to better localize differences in perfusion. This emphasizes the wealth of information that can be obtained by examining individual muscle groups. For example, seeing which muscle regions are affected in individual patients could help guide therapy, for recommendations for particular structured exercise could then be made to help maximize chances of functional improvement. Furthermore, results of calf imaging could be correlated with blood flow territories to the foot, which is of great importance in critical limb ischemia. Correlating the results with

foot ulceration and limb ischemia could help guide management, therapy, revascularization procedures, and predict outcomes. Additionally, it would be useful to delineate differences in muscle perfusion during exercise versus pharmacological stress testing, as well as to differentiate between various types of pharmacological stress testing.

The muscles in the calves and the lower leg include the triceps surae ("three-headed calf," composed of the two-headed gastrocnemius muscle and soleus muscle) and tibialis anterior, tibialis posterior, and fibularis. The gastrocnemius and soleus are both connected to the foot through the Achilles tendon. The gastrocnemius gives off two heads attaching to the base of the femur directly above the knee. These origins and insertions allow for plantar flexion at the ankle joint, as well as flexion at the knee joint. The soleus is the deeper mass of muscle that attaches to the superior posterior area of the tibia. Together with the gastrocnemius, it allows for plantar flexion of the foot, in addition to stabilizing the tibia on the calcaneus and thus limiting forward sway.

The tibialis anterior originates in the lateral surface of the tibia and inserts into the bones of the foot. It acts to dorsiflex and invert the foot. It stabilizes the ankle as the foot hits the ground during the contact phase of walking. The tibialis posterior originates on the inner posterior borders of the tibia and fibula, and is the stabilizing muscle of the lower leg. It also helps with inversion and plantar flexion of the foot. The fibularis muscles are a group of three muscles - the fibularis

longus, brevis, and tertius, which originate on the fibula and insert on the
metatarsals. These muscles are located in the lateral and anterior compartment of
the foot and help with eversion, plantar flexion, and dorsiflexion.

By knowing the insertion and origin and function of each of these muscles, it is
possible to understand which of these are used in certain exercises. For example,
some of the best sports for building the calves include sprinting and running.
Additionally, cycling, especially at high pedaling speeds, helps to build the calf
muscles. Importantly, the soleus is composed of mostly type I, or slow-twitch,
muscles. It is made of approximately 60-100% of type I fibers and is thus good
for repetitive exercises which use oxygen. In contrast, the gastrocnemius has
approximately 57% of its fibers as type II, or fast-twitch, muscle fibers,[16] and thus
is best for sprints. Unlike most other activities, during cycling, the gastrocnemius
muscles are active for a long period of time, which helps explain why cycling at
high speeds is particularly helpful for exercising the gastrocnemius. Knowledge
of the composition of fiber type for each muscle group is important to help
determine which exercise would be best for therapy to improve the PAD in
particular patients.

Statement of Purpose

Hypothesis

SPECT/CT rest imaging in PAD may be sufficient to evaluate disease in critical limb ischemia, although stress imaging will be required to detect PAD in asymptomatic patients or patients with claudication. Exercise stress testing is more accurate than is pharmacological stress testing for detecting PAD, as the legs are being stressed directly. SPECT/CT is a more sensitive and specific method of detecting peripheral arterial disease in diabetic patients than is the ankle-brachial index, as microvascular perfusion can be visualized despite arterial calcifications.

Specific Aims

<u>Aim 1:</u> To translate image analysis tools previously developed and validated in preclinical models of PAD to patients, evaluating the reproducibility of the approach, and feasibility for clinical application.

<u>Aim 2:</u> To evaluate and compare changes in lower extremity perfusion at stress and rest in patients with diabetes, PAD, and those with indeterminate ABIs.

Methods

This study was performed with Human Investigations Committee (HIC) approval, with informed consent of patients. Lower extremity tissue perfusion was evaluated in patients using ^{99m}Tc-tetrofosmin SPECT/CT imaging. Patients that were clinically indicated to undergo myocardial perfusion imaging at rest and during exercise or pharmacological (adenosine or regadenoson) stress were asked to participate in the study. The ABI of each patient was obtained using the standard American Heart Association guidelines before or between their scans. Either preceding or following the rest and/or stress myocardial perfusion imaging, patients underwent rest and/or stress imaging, respectively, at the level of the calf using a conventional hybrid SPECT/4-slice CT imaging system (Infinia "Hawkeye", GE Healthcare). All lower extremity SPECT/CT imaging was done using the ^{99m}Tc-tetrofosmin that was previously injected for myocardial perfusion imaging. Therefore no additional radioisotope administration was required for these studies.

Lower Extremity SPECT/CT Acquisition

Image analysis tools previously developed in murine and porcine models of hind limb ischemia were used to analyze and quantify regional skeletal muscle perfusion in SPECT/CT images. The system software (GE, Xeleris) was used to co-register CT and SPECT images to correlate radiotracer uptake seen on the

SPECT images with the anatomical regions observed from CT images. If a patient

moved between SPECT and CT acquisitions, the co-registration tool would allow

for the areas outlined in red (demonstrating the maximal areas of radioactivity) to

be registered with the CT images. It also allowed for attenuation correction so that

scattering problems due to differences in tissue density were minimized. The

software VH Dissector Pro provided actual anatomical correlation on gross cross-

sections to the cross-sections seen on the CT images.

SPECT/CT Image Quantification

The axial CT and attenuation-corrected SPECT images were opened in OsiriX, as

shown in panels a and b of Figure 1. In this program, ROIs were drawn around

each respective muscle group, including the tibialis anterior, tibialis posterior,

fibularis, soleus, and gastrocnemius. Panel c of Figure 1 illustrates the ROIs that

were drawn on a CT image of the calves of Patient E at rest. After all of the

regions were drawn on CT images throughout the entire length of the calf, these

ROIs were copied onto the SPECT images, as is seen on panel e of Figure 1. With

this technique, the CT images were used to delineate the anatomical boundaries of

each muscle group, and copying the ROIs onto the respective SPECT images

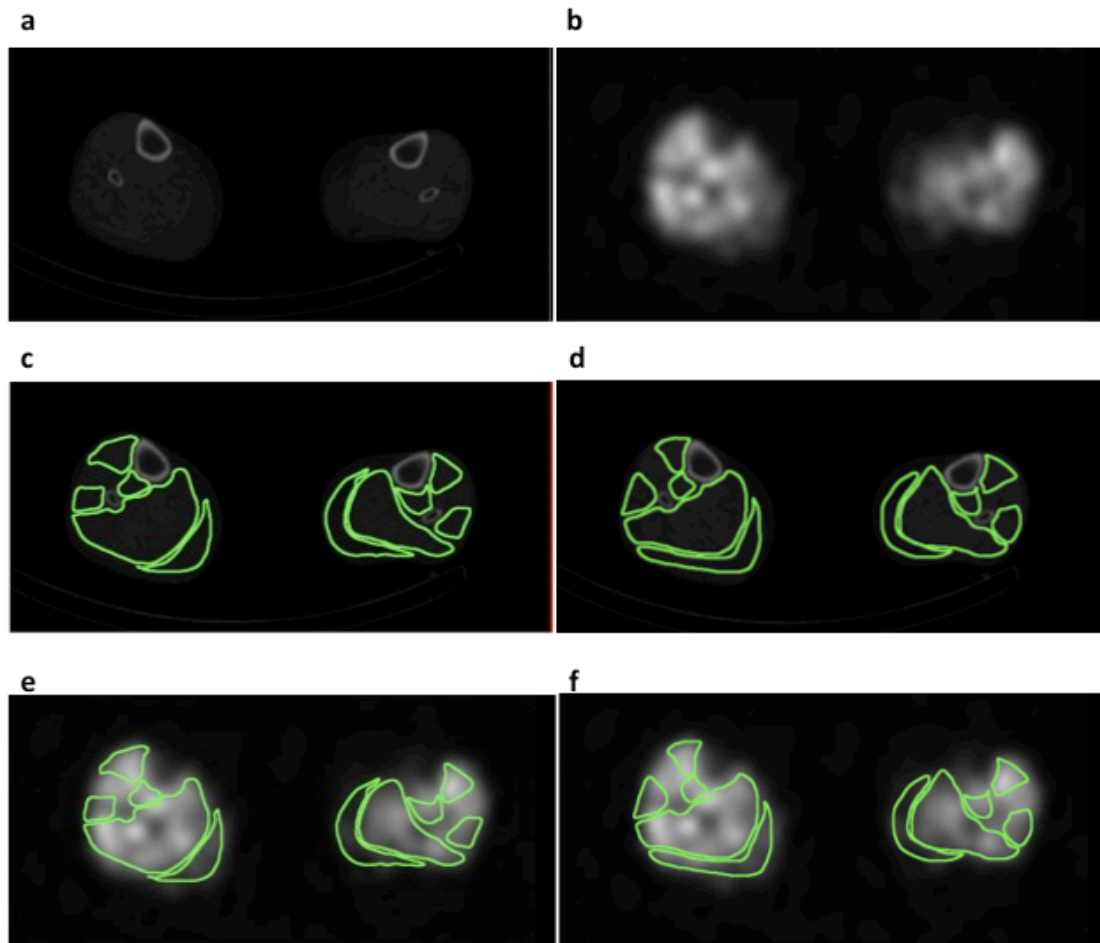allowed the radioactivity for each muscle region to be measured.

Figure 1. ROIs drawn on axial images of the calves of Patient E at rest.
Panel a (CT image), b (SPECT image), c (CT image with first set of ROIs), d (CT image with second set of ROIs), e (SPECT image with ROIs copied from first set of ROIs), f (SPECT image with ROIs copied from second set of ROIs).

After ROIs were created for each CT and SPECT image, OsiriX would create a volume of interest (VOI) for each muscle group by combining the ROIs over the length of the calf. From this VOI, it was possible to compute the average intensity value for each muscle group, which correlates with the amount of radioactivity per volume of muscle in each muscle group. The injected dose of ^{99m}Tc-tetrofosmin was also corrected for decay using the decay equation $A=A_o*e^{\wedge(-}$

$^{.693t/T1/2)}$, by incorporating the time between injection and scanning. Finally, the total intensity value for each muscle group was divided by the volume of the VOI and by the corrected injected dose to output the main variable analyzed in this study.

The severity of the diabetes and symptoms for each patient were also tracked closely in order to correlate these factors with imaging results. These factors included HbA1c level, duration of diagnosis, insulin dosing and medications, presence of claudication or foot ulcers, body mass index, cholesterol and triglyceride levels, smoking status, presence of retinopathy, nephropathy, neuropathy, or cerebrovascular events, cardiovascular complications, and any metabolic disturbances.

Patient Recruitment

29 patients were scanned for this study. The researcher Sumarriva recruited, consented, and oversaw the scanning of 20 of these patients and also obtained ABI measurements and additional information regarding medical conditions, diabetes status, etc. 12 patients were analyzed for the purposes of this study, including 4 that were diabetic and 3 that had PAD. (Of these 12, the researcher Sumarriva analyzed 7.) 2 of these 3 patients with PAD had been previously diagnosed with PAD, while 1 was diagnosed using the toe-brachial index obtained later on in the study. Of the 12 patients, 5 patients had 2 sets of ROIs drawn by

the same observer, so as to allow for analysis of the reproducibility of the

methodology. 6 of these 12 patients had both rest and stress imaging.

Statistical Analysis

Statistical analyses were performed using SPSS Statistics software. Significance

was determined with P value <0.05, and using a mixed model regression.

Results

	All combined (n=12)	Control group (n=7)	Diabetic group (n=4)	PVD group (n=3)
Average age and range	57.9 (42-74)	54.9 (42-74)	64.3 (59-72)	64.7 (60-72)
Gender	M=8, F=4	M=4, F=3	M=2, F=1	M=2, F=1
Average BMI (kg/m^2) and range	28.6 (19.5-39.5)	29.4 (19.5-39.5)	29.0 (24.8-31.4)	25.7 (21.5-30.7)
Co-morbidities		CAD (2), HTN (5), HLD (3), CKD (1), Raynaud's (1)	HTN (4), PVD (2), HLD (4), CKD (2), carotid artery stenosis (1), CHF (1), peripheral neuropathy (1), MI (1), CAD (1)	DM (2), HTN (2), HLD (2), CKD (2), CHF (1), carotid artery stenosis (1) , peripheral neuropathy (1)
Average R ABI and range	1.13 (0.63-1.45)	1.20 (0.9-1.4)	0.96 (0.63-1.45)	0.87 (0.63-1.18)*
Average L ABI and range	1.19 (0.92-1.7)	1.19 (0.95-1.7)	1.16 (0.92-1.36)	1.14 (0.92-1.3)*

Table 1. Group characteristics. CAD = coronary artery disease, HLD = hyperlipidemia, HTN = hypertension, DM = diabetes mellitus, CKD = chronic kidney disease, MI = myocardial infarction. * indicates that one patient in the PAD group had normal or indeterminate ABI values, but TBI values diagnostic of PAD.

Table 1 demonstrates the characteristics of the 12 patients that were scanned and

analyzed. Notably, the mean ABI values for the diabetic group were close to the

cutoff of 0.90 for the right side, and they met the cutoff value for the right side of

the PAD group.

Patient	Gender	Age	BMI (kg/m^2)	Co-Morbidities	Smoking History	R ABI	L ABI	Rest	Stress
Patient A	M	55	22.1	Raynaud's	Former smoker	1.28	1.22		X (E)
Patient B	M	59	31.4	DM, HTN, HLD		1.45	1.36		X (E)
Patient C	F	62	30.7	PVD, T2DM, HTN, HLD, CHF, b/l carotid artery stenosis, chronic renal insufficiency	Former smoker	0.63 (0.88 from outside clinic)	0.92 (1.17 from outside clinic)	X	
Patient D	M	58	33.2	CAD, HTN, HLD, chronic kidney disease, ulcerative colitis, gout	Former smoker, 45 pack-years	1.26	0.96	X	
Patient E	F	74	37.5	HTN, HLD, paroxysmal AFib, b/l knee implants	60+ pack-years	1.16	1.16	X	X (P)

Table 2. Patient demographics for intra-observer reproducibility analysis.
E = Exercise stress, P = Pharmacological stress

It is important to note from Table 2 that several of the patients do not exactly meet

the cutoff value diagnostic of PAD or of an indeterminate value, but that they are

close to the cutoff. Examples are Patients A and D.

Patient	Gender	Age	BMI (kg/m^2)	Co-Morbidities	Smoking History	R ABI	L ABI	Stress	Rest
Patient F	F	42	28.0	HTN, heart palpitations	Non-smoker	1.14	1.22	X (E)	
Patient G	M	72	24.8	PVD, DM, HTN, HLD, chronic renal failure, peripheral neuropathy, R foot infection	Former smoker	0.79	1.19		X
Patient H	F	46	39.5	CAD, HTN, HLD, depression	Former smoker, 5 pack-years	1.29	1.70	X (E)	X
Patient I	M	53	19.5	Cocaine abuse, polysubstance abuse	Smoker	0.90	1.15	X (E)	X
Patient J	M	56	26.2	HTN, angina of effort	Non-smoker	1.40	0.95	X (E)	X
Patient K	M	60	21.5	Dyspnea	Smoker, 40 pack-years	1.18 (TBI 1.02)	1.30 (TBI 0.56)	X (E)	X
Patient L	M	65	31.8	DM, CAD, HTN, HLD, MI, cholelithiasis	Non-smoker	1.08	1.20	X (E)	X

Table 3. Patient demographics for additional patients in rest vs stress analysis.

CT and SPECT Images

CT attenuation and SPECT images were obtained for each patient, resulting in coronal, sagittal, and axial cross-sections. The imaging software allowed for co-registration of SPECT and CT images, additionally allowing for attenuation correction. Figures 1 and 2 illustrate hybrid imaging of the calves of Patient E in the three planes during rest and stress.
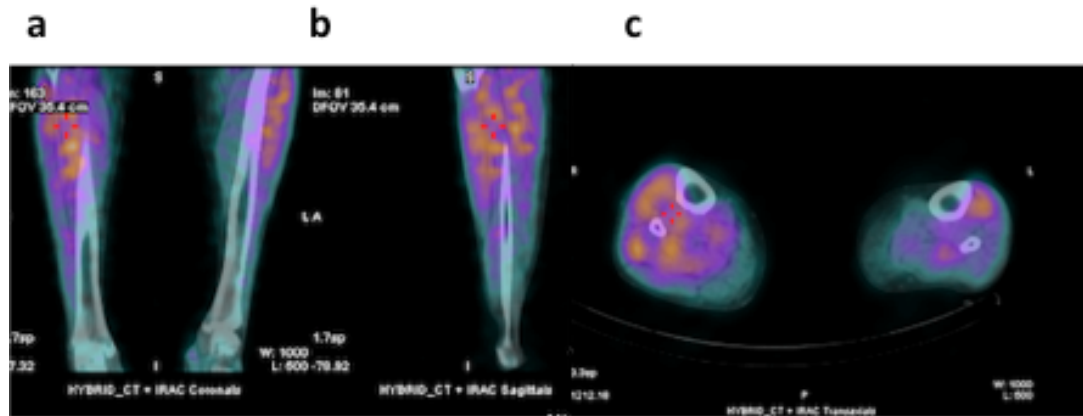
Figure 2. Hybrid SPECT/CT cross-sectional images of the calves of Patient E at rest. Panel a (coronal section), b (sagittal section), and c (axial section).
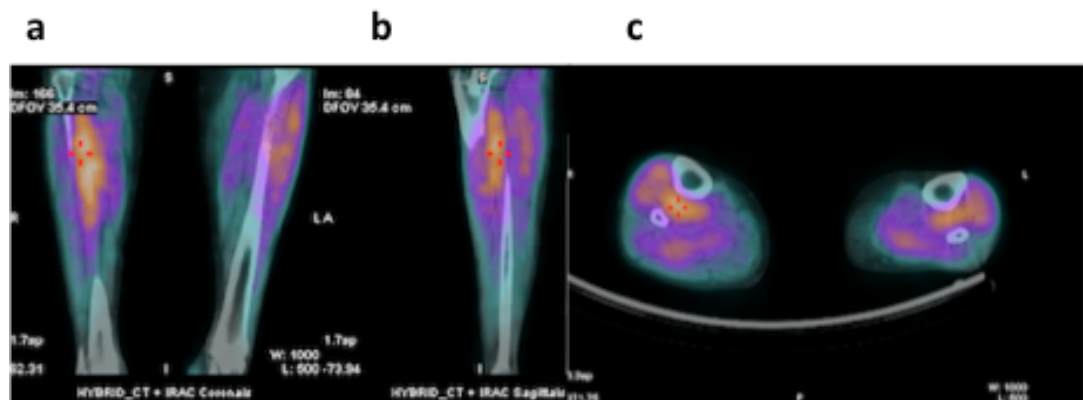

Figure 3. Hybrid SPECT/CT cross-sectional images of the calves of Patient E at stress. Panel a (coronal section), b (sagittal section), and c (axial section).

Registration of Radioactivity on SPECT and CT Images

Panels a, b and c on Figure 4 have the maximal areas of radioactivity outlined in red on coronal, sagittal, and axial SPECT images of the calves of Patient E at rest. Panels d, e, and f on Figure 4 show the radioactivity from the SPECT imaging correlated to the corresponding areas on the coronal, sagittal, and axial CT images of the calves of Patient E at rest.
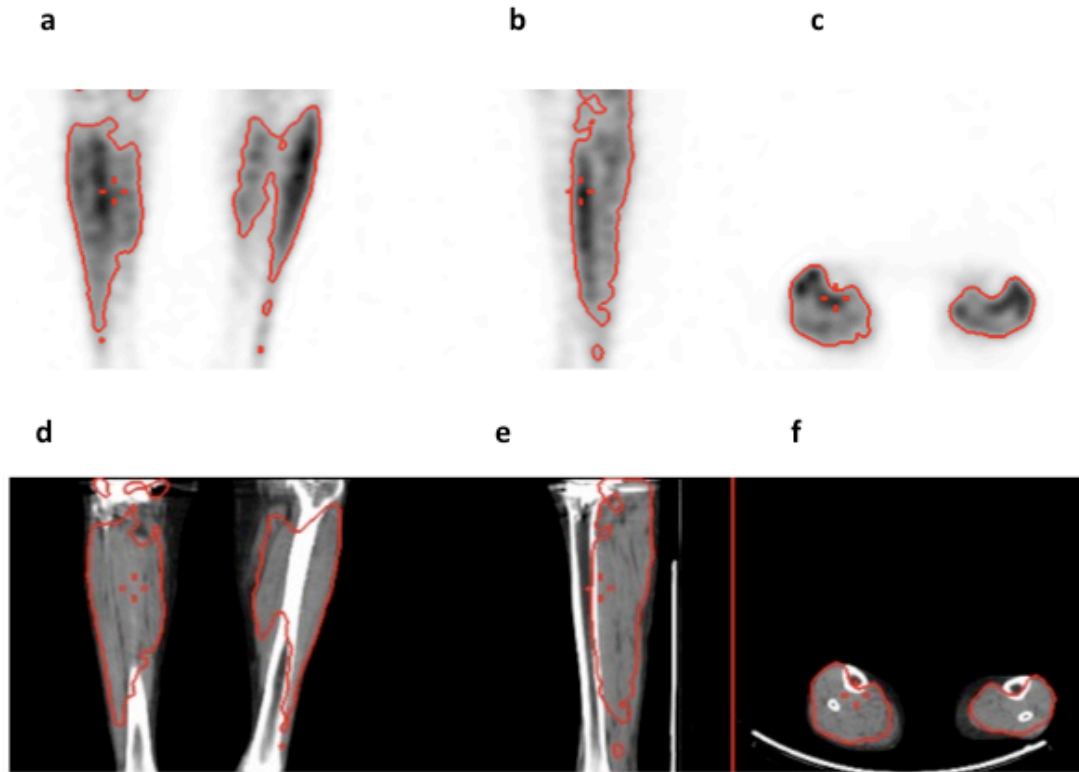
Panels a, b, and c on Figure 5 show the maximal areas of radioactivity outlined in red on coronal, sagittal, and axial SPECT images of the calves of Patient E after pharmacological stress. Panels d, e, and f on Figure 5 show the radioactivity from the SPECT imaging correlated to the corresponding areas on the coronal, sagittal, and axial CT images of the calves of Patient E after pharmacological stress.

Figure 4. Registration of radioactivity on SPECT and CT images on the calves of Patient E at rest. Panel a (coronal), b (sagittal), and c (axial) sections on SPECT images. Panel d (coronal), e (sagittal), and f (axial) sections on CT images.
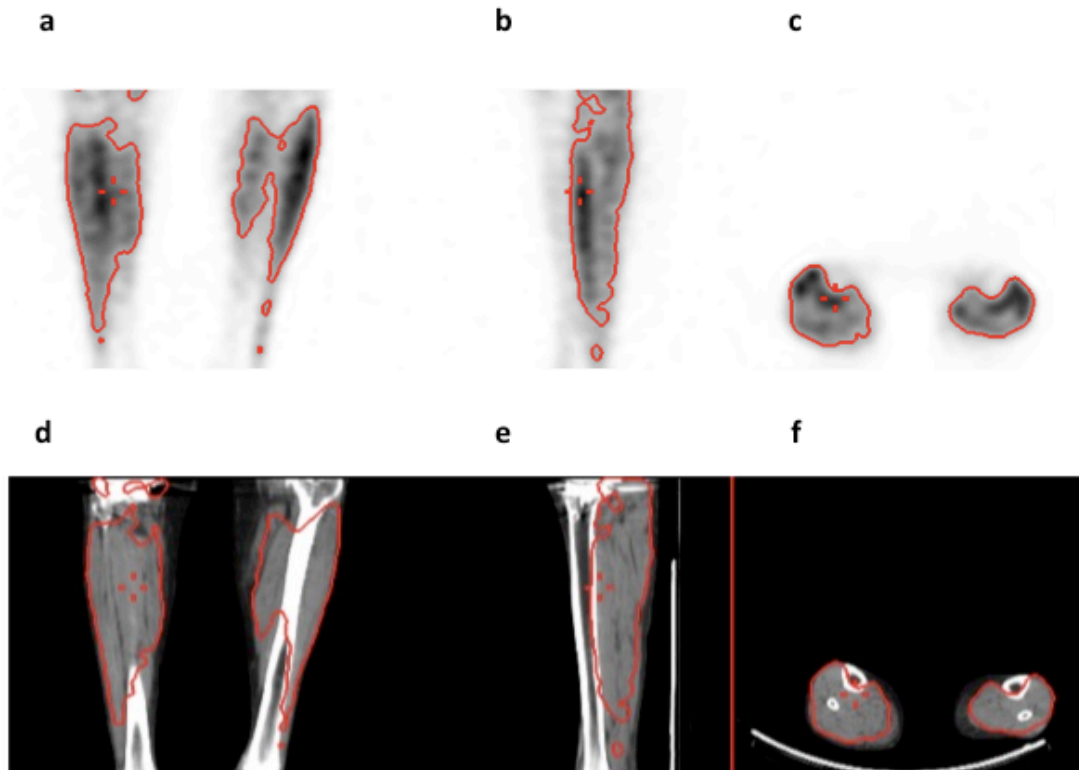
Figure 5. Registration of radioactivity on SPECT and CT images on the calves of Patient E at stress. Panel a (coronal), b (sagittal), and c (axial) sections on SPECT images. Panel d (coronal), e (sagittal), and f (axial) sections on CT images.

Regions of Interest on CT and SPECT Images

In order to determine the reproducibility of the methods, two sets of ROIs were drawn for each of the 5 patients analyzed in this study. The same researcher drew these at two separate times, without comparing the two sets of images when drawing the ROIs. Panel d of Figure 1 (above) illustrates the same axial CT slice as seen in panel c of Figure 1, to allow for comparison of ROIs from each set of drawings. Panel f of Figure 1 illustrates the copied ROIs from the CT images in panel d of Figure 1.

Panels a through f of Figure 6 demonstrate the corresponding images for stress as for the rest images seen in Figure 1. As seen in panels a and b of Figure 7, it was possible to correlate any cross-section of rest imaging with its corresponding cross-section from stress imaging, regardless of the change in time or position that took place between the two sets of scans.
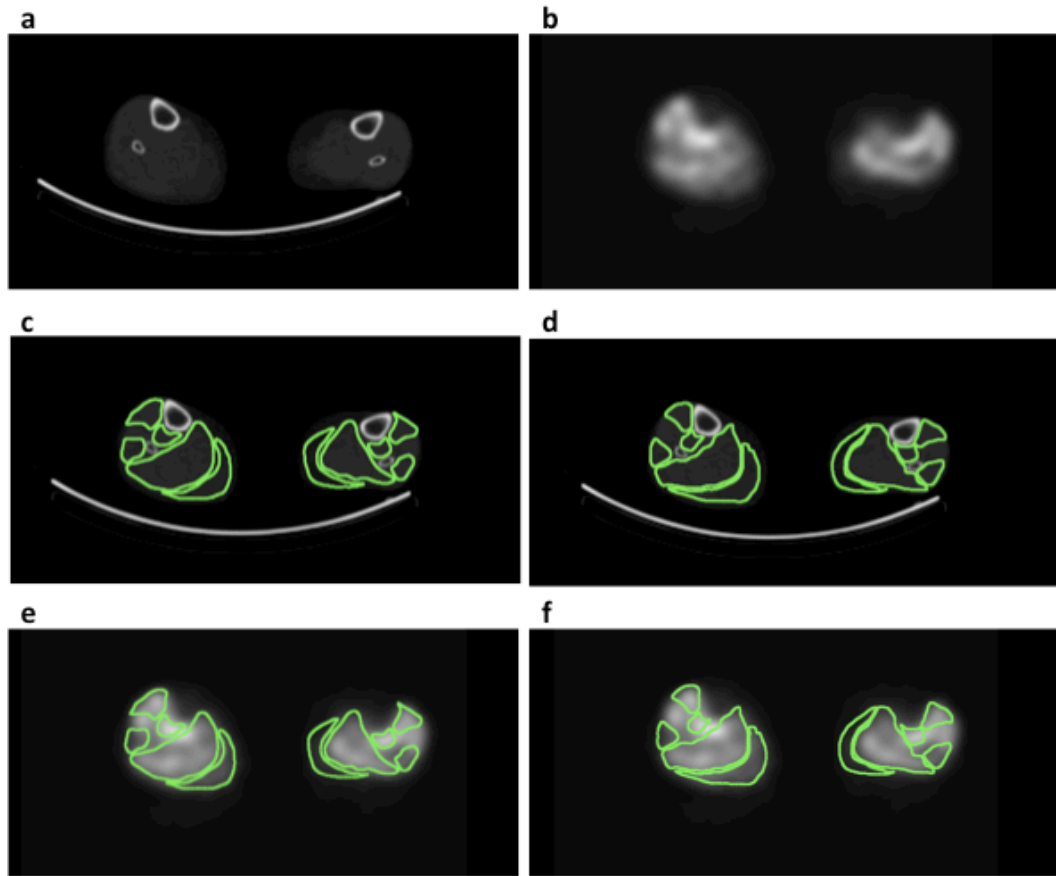
Figure 6. ROIs drawn on axial images of the calves of Patient E at stress.
Panel a (CT image), b (SPECT image), c (CT image with first set of ROIs), d
(CT image with second set of ROIs), e (SPECT image with ROIs copied from
first set of ROIs), f (SPECT image with ROIs copied from second set of ROIs).
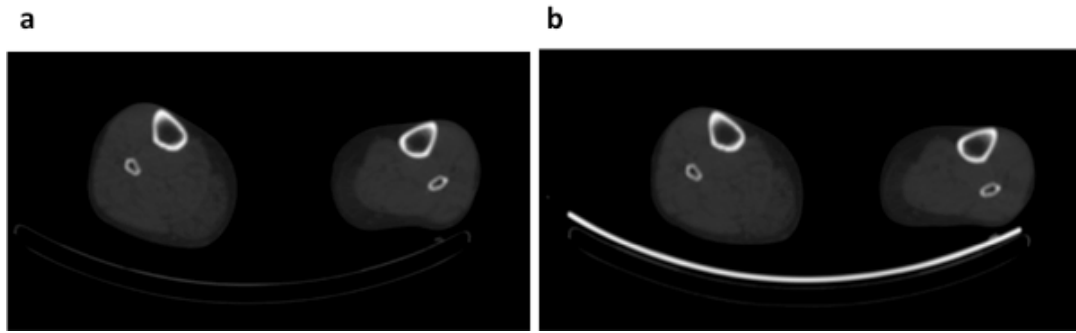
Figure 7. Comparison of corresponding rest (panel a) and stress (panel b) axial images of the calves of Patient E. Panels a (CT slice 32 of 119) and b (CT slice 40 of 119).

Intra-Observer Variability for Patients A through E

To compare the two sets of ROIs drawn for each patient, the two values obtained

for intensity/(volume*corrected injected dose) for each muscle group were plotted

on x and y axes and a trend line drawn, as shown in Figures 8 and 10.

Additionally, Bland-Altman plots were created, as in Figures 9 and 11. These

plots shows the variability between the two sets of ROIs by comparing the

average intensity per volume per corrected injected dose, or the main output

variable in the study, with the difference between the two values. The plots thus

demonstrate the intra-observer variability for the two sets of ROIs drawn for each

patient. The mean and standard deviations are included on the plots, and it is

important to note that Patient B consistently had variability greater than 1

standard deviation above the mean, indicating greater likely error between the two

sets of values. Notably, Patient E had both rest and stress imaging of the calves,

so four sets of ROIs were drawn for this patient. Patient E was the only patient of

the 5 that had both rest and stress imaging done. Additionally, it is apparent in

Figure 11 that at greater corrected intensities per volume per injected dose, there
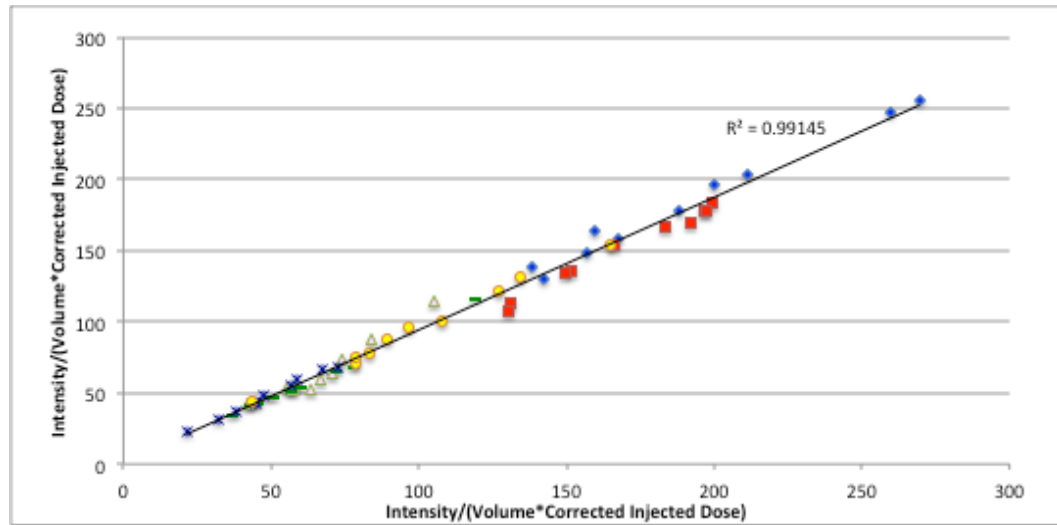
is greater variability.

Figure 8. Comparison of two values for intensity/(volume*corrected injected dose) for each patient. Blue diamond = Patient A, red square = Patient B, green triangle = Patient C, green minus sign = Patient D, purple cross = Patient E (Rest), yellow circle = Patient E (Stress). R^2 = 0.99145.
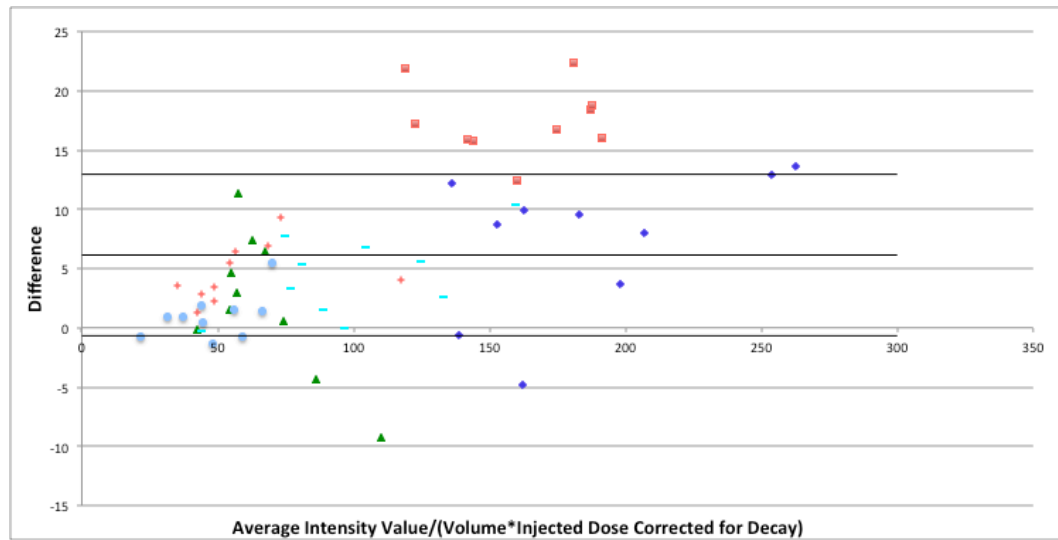
Figure 9. Intra-observer variability divided among Patients A through E. Bland-Altman plot for the muscle groups of Patients A through E. Purple diamond = Patient A, red square = Patient B, green triangle = Patient C, red plus sign = Patient D, light blue circle = Patient E (Rest), aquamarine minus sign = Patient E (Stress).
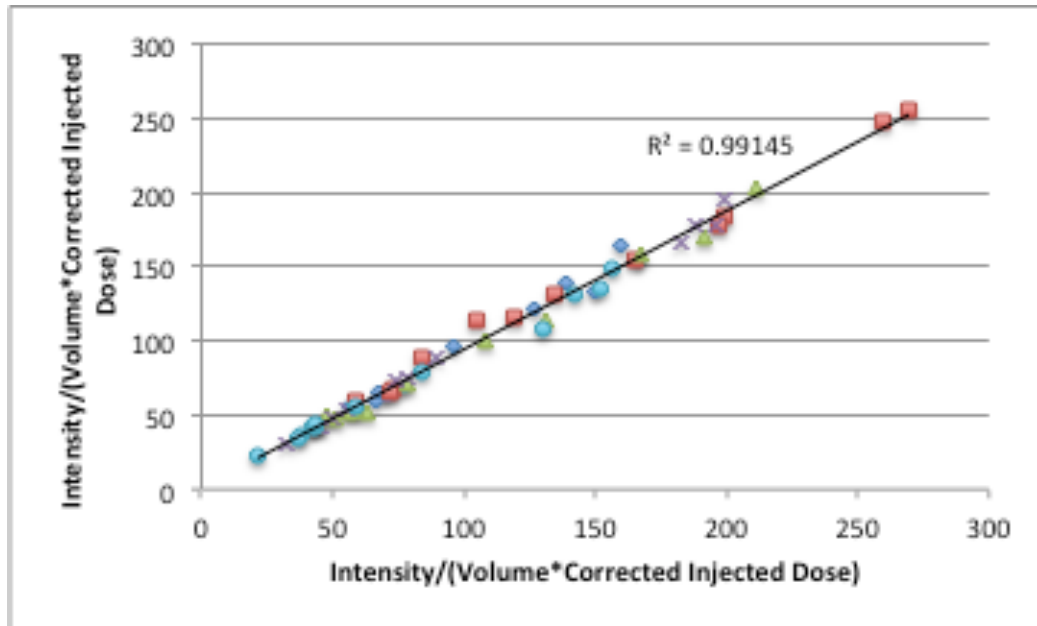
Figure 10. Comparison of two values for intensity/(volume*corrected injected dose) for each muscle group. Left and right sides grouped together. Blue diamond = tibialis anterior, red square = tibialis posterior, green triangle = fibularis, purple cross = soleus, blue circle = gastrocnemius. $R^2 = 0.99145$.
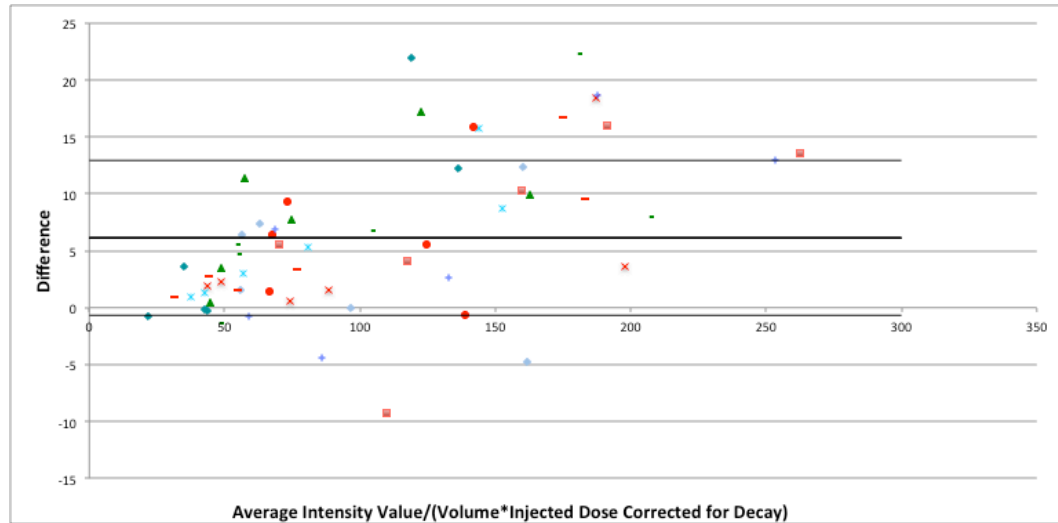
Figure 11. Intra-observer variability divided among muscle groups. Bland-Altman plot for patients A through E. Purple diamond = R tibialis anterior, red square = R tibialis posterior, green triangle = R fibularis, red x = R soleus, aquamarine x = R gastrocnemius, red circle = L tibialis anterior, purple plus sign = L tibialis posterior, green horizontal hash mark = L fibularis, red minus sign = L soleus, teal diamond = L gastrocnemius.

Results for ROIs

Panels a through f of Figure 12 show the intensity per volume per corrected

injected dose that was obtained for each muscle group from each set of ROIs.

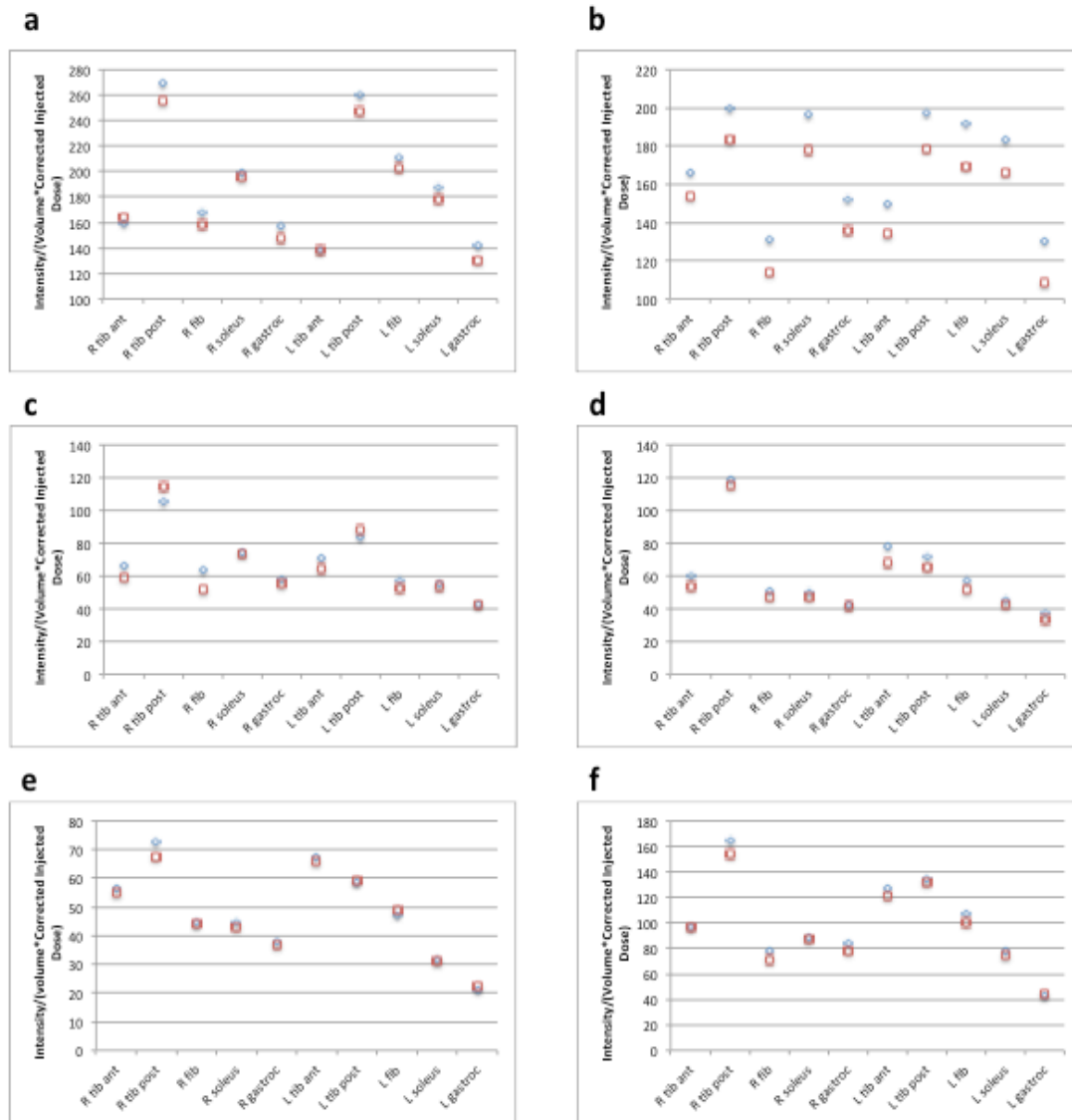Data for each patient is included on individual graphs.

Figure 12. Intensity/(volume*corrected injected dose) for each muscle group, for each set of ROIs, per subject. Panels a (Patient A), b (Patient B), c (Patient C), d (Patient D), e (Patient E – Rest), f (Patient E – Stress). Blue diamond = first set of ROIs, red square = second set of ROIs.

Stress and Rest Results Subdivided into Muscle Groups

Figure 13 demonstrates the intensity per volume per corrected injected dose for each of the muscle groups for the 6 patients analyzed at both rest and stress. Values are consistently higher for stress than for rest for each muscle group. Figure 14 illustrates the intensity per volume per corrected injected dose for each of the muscle groups for the patients analyzed at exercise stress, subdivided into control patients vs PAD, indeterminate ABI, and diabetic patients. At exercise stress testing conditions, there is higher perfusion in the controls than in patients with possible or likely vascular disease.

Figure 15 shows the relative values of intensity per volume per corrected injected dose at rest for each of the muscle groups, subdivided into control patients vs PAD, indeterminate ABI, and diabetic patients. Notably, the values are higher for the patients with possible or likely vascular disease than for the control patients. Figure 16 then shows the fold-increase in stress versus rest values for the 12 patients analyzed.
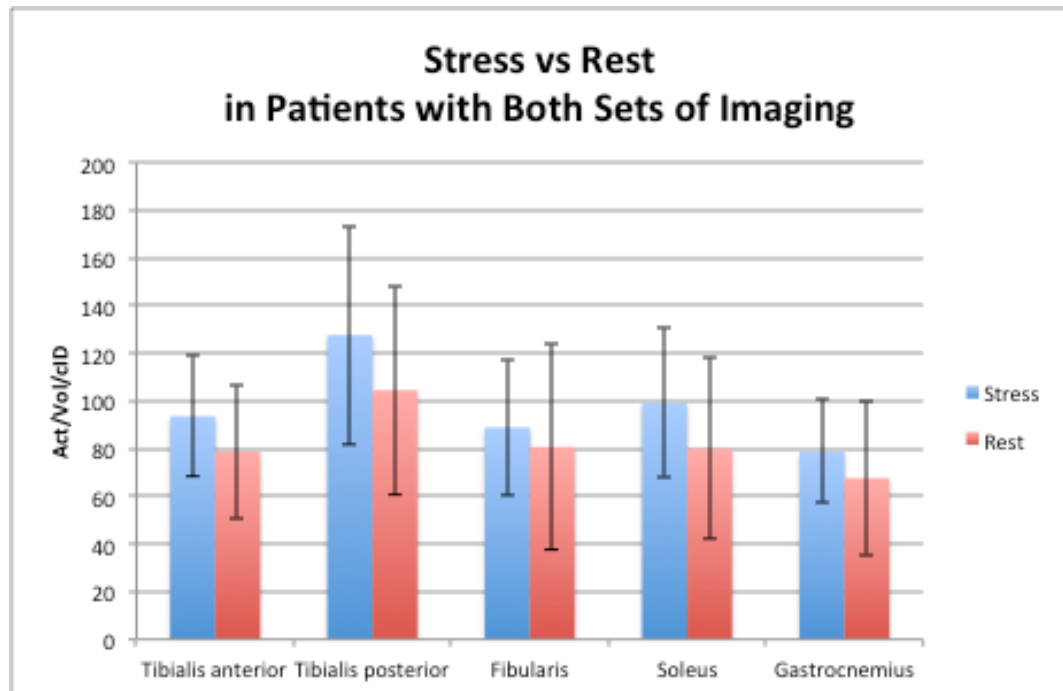
Figure 13. Stress vs Rest Comparison in Patients with Both Sets of Imaging (Patients E, H, I, J, K, L) . Columns show the mean (N =6), error bars are +/- standard deviation.

Using the program SPSS Statistics, it was found that stress vs rest perfusion

indices were statistically different for the 6 patients that had both stress and rest
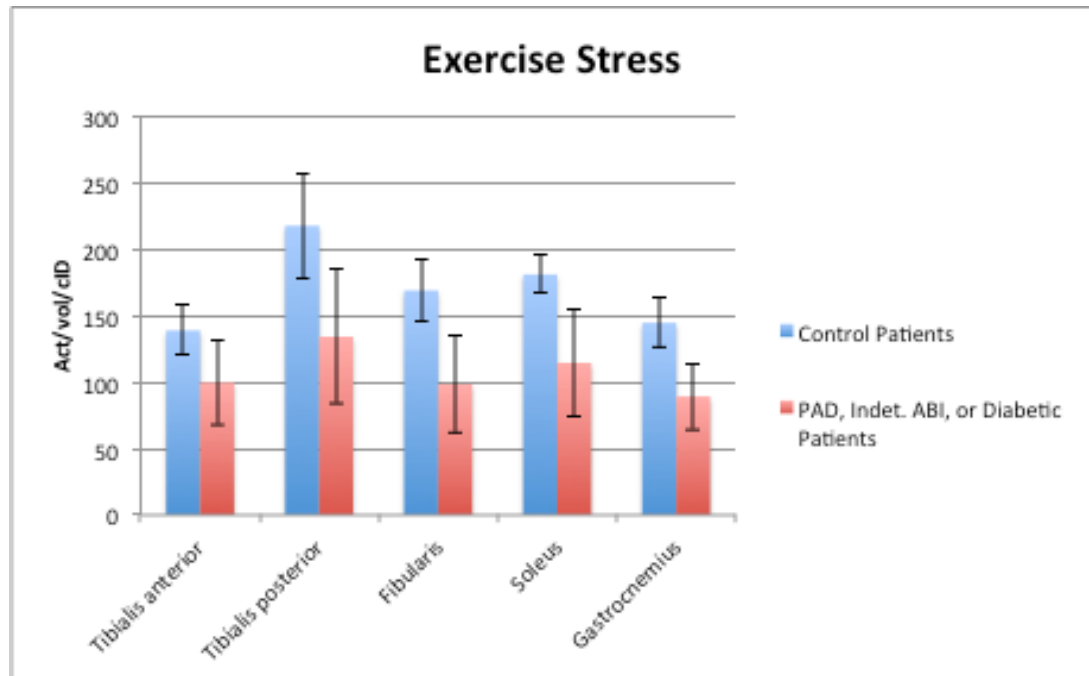
imaging (P=0.001).

Figure 14. Intensity per volume per corrected injected dose for patients under exercise stress, subdivided into controls (n=2) vs PAD, indeterminate ABI, or diabetic patients (n=6). Data is divided into left and right individual muscle groups. Columns show the mean, error bars are +/- standard deviation.
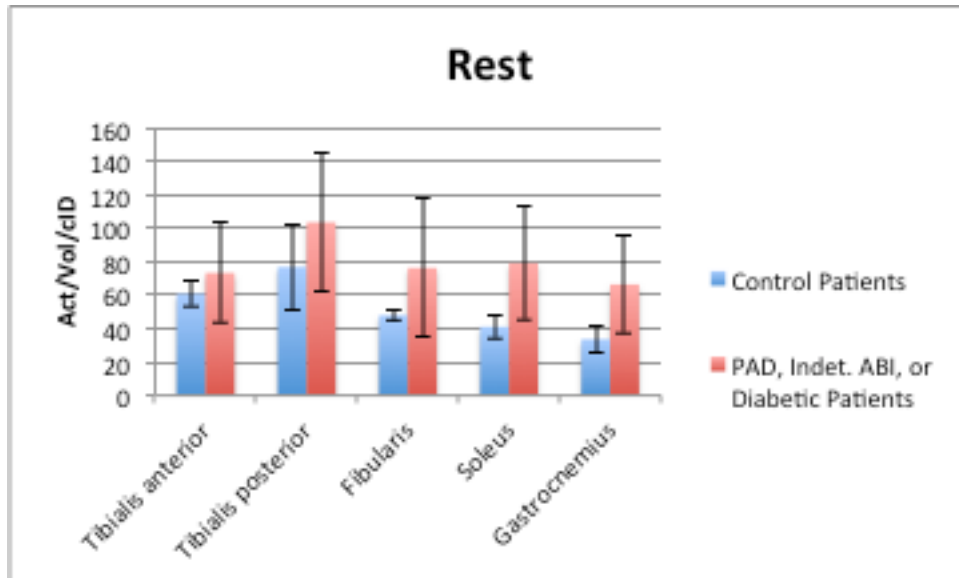
Figure 15. Comparison of intensity per volume per corrected injected dose at rest for control patients (n=2) vs PAD, indeterminate ABI, or diabetic patients (n=7) . Data is divided into individual muscle groups. Columns show the mean, error bars are +/- standard deviation.
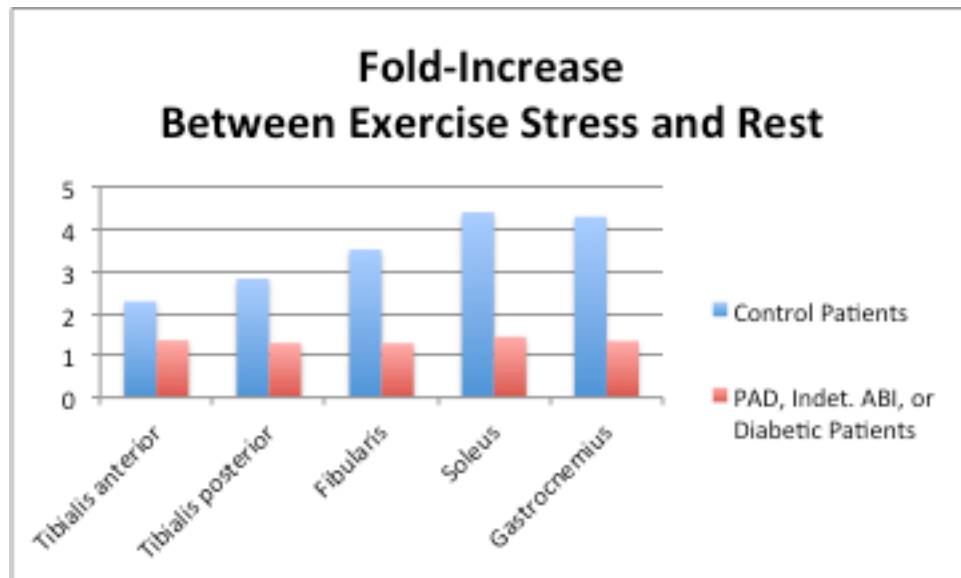
Figure 16. Fold-increase between average stress and rest values, subdivided into controls (n=4) vs PAD, indeterminate ABI, or diabetic patients (n=8). Data is divided into individual muscle groups.

Discussion

This study translated methods previously developed for quantitative analysis of hybrid SPECT/CT images of lower extremity perfusion in murine[17] and porcine[18] models of hindlimb ischemia to clinical SPECT/CT images of the lower extremities of patients referred for stress/rest cardiac perfusion imaging. This pilot clinical population included a range of patients with and without suspected PAD. Though previous clinical studies have used a range of radiotracer-based imaging modalities to quantify perfusion in the lower extremities of patients[5,14], no study had previously analyzed hybrid SPECT/CT images with the goal of analyzing

changes in perfusion to specific lower extremity muscle groups following both exercise and pharmacological stress. Any changes in radiotracer perfusion will reflect both abnormalities in the microcirculation as well as the larger arteries, offering a potential advantage over ABIs particularly in diabetic patients with a high incidence of microvascular disease.

We demonstrated that this quantitative hybrid SPECT/CT approach was not only feasible for evaluating perfusion is specific lower extremity muscle groups of patients but highly reproducible. The error in the estimation of muscle specific perfusion is primarily introduced from semi-automatically drawing the volumes of interest on muscles whose delineation depends on the resolution of the CT scan, although may also be affected by registration of the SPECT and CT images. Since this study used a low radiation dose CT attenuation scan after each SPECT acquisition (to avoid introducing additional risks to the subjects involved), the muscles on each CT slice were not very well-delineated, and thus the VOIs were not reproducible with incredibly high precision. However, as seen in Figures 1 and 6, the 2-dimensional ROIs drawn were relatively comparable. As can also be seen in panels c and d of Figure 5, the gastrocnemius and the soleus (the two muscles located most inferiorly in the images) were the hardest muscles to delineate on the CT scans, particularly in some patients. However, this difficulty is not apparent on Figure 10, as there appears to be no systematic bias either for or against any one muscle group with regard to reproducibility. Thus, according to Figure 9, there was no greater difficulty or ease in drawing any particular muscle

group for the researcher that drew both sets of ROIs. Furthermore, the panels in Figure 12 show that the main output variable (intensity per volume per corrected injected dose) was very similar in value and in pattern between the two sets of ROIs for some of the subjects.

Figure 9 illustrates the intra-observer variability for each patient, instead of being grouped by muscle group. There is clearly a systematic bias present, as the differences (y-values) varied considerably from one patient to another. This may be due to several factors. One of the clearest factors to notice is the order in which the ROIs were drawn between patients. For example, Patient B, who has the greatest difference values, was one of the first subjects for whom this researcher drew ROIs. The second set of ROIs for each of these patients, with the exception of Patient E, was drawn after several more weeks of experience than when drawing the first set of ROIs. In the same regard, Patient E had the smallest difference values for both stress and rest sets of ROIs. This trend likely exists because this patient was the last one on whom ROIs were drawn, and thus the researcher had the most experience in this, in addition to similar amounts of experience for when drawing each set (each set of ROIs for Patient E were drawn with only a few days' difference in experience). Thus, there is an improvement in using this method depending on the amount of training. Therefore, for future studies, when requiring new researchers to learn this method, the new researcher should have sufficient practice before beginning to analyze data that would be used in the study.

Another factor that may account for the systematic bias present from patient to patient is the fact that muscles were delineated with different degrees of markings between the muscle groups depending on the age and fitness level of the patient. For example, Patient A was a very fit individual in his fifth decade of life who participated in long-distance running (as learned by history), and his muscle groups were packed very closely together. In contrast, Patient E was a more sedentary individual in her seventh decade of life, with muscles that were not packed very tightly together. She thus had a greater number of landmarks on the CT images to help distinguish one muscle group from another. Therefore, in general, the older the individual, the more it seemed that the muscles were easier to analyze.

Figure 13 shows that perfusion between rest and stress differ, even though 5 of these 6 patients had either PAD, indeterminate ABIs, or diabetes. Had more control patients been included in this figure (and been analyzed at both stress and rest), the difference between stress and rest would be even greater, a trend that is seen in Figure 16. Figure 14 demonstrates a greater perfusion at stress testing in the control patients than in patients with PAD, indeterminate ABIs, or diabetes, while in Figure 15, there is a greater perfusion at rest for the latter group. This can be partially accounted for with reasoning used in a study by Burt et al,[19] in which it was hypothesized that muscles supplied by a completely or severely occluded arterial supply had more ^{201}Tl uptake than those supplied by normal vessels if the

isotope injection was given with a slight delay (about 4 minutes after cessation of exercise). They stated that muscles supplied by stenotic vessels have delayed maximal blood flow and a prolonged vasodilatation, because they are supplied by high-resistance collateral roots. While the study by Burt used ^{201}Tl, the study by Bajnok et al.[15] showed a similar paradoxical uptake by ^{99m}Tc-sestamibi. It is possible that the radiotracer used in the present study also shows a paradoxical uptake.

It is also important to note that Figure 16 shows that the fold-increase between exercise stress and rest was greater for the control patients than those with PAD, indeterminate ABIs, or diabetes. This could indicate a greater amount of perfusion reserve for control patients than for the second group. Certainly, more patients would need to be scanned and analyzed in order to reach clinically significant conclusions. Further analysis would also delineate differences in the individual muscle groups, which is the novel approach that was used in this study.

In future studies, this quantitative SPECT/CT perfusion methodology can be used for a host of clinical applications; including the evaluation of stress induced changes in perfusion in the lower extremities of patients with diabetes mellitus or peripheral arterial disease as compared to control subjects. This hybrid non-invasive imaging approach is currently being applied in a larger number of patients in order to evaluate the potential advantage over ABIs for the early detection of microvascular disease in diabetic patients. As this methodology

demonstrates acceptable reproducibility following a sufficient amount of training, this approach could be a novel method to assess the pathophysiological changes in individual muscle groups of subjects. In addition, this method could be used to compare the different types of stress testing used, including exercise stress testing or pharmacological stress testing.

References

1.   Ostchega Y, Paulose-Ram R, Dillon CF, Gu Q, Hughes JP. Prevalence of peripheral arterial disease and risk factors in persons aged 60 and older: data from the National Health and Nutrition Examination Survey 1999-2004. Journal of the American Geriatrics Society 2007;55:583-9.

2.   Kim ES, Wattanakit K, Gornik HL. Using the ankle-brachial index to diagnose peripheral artery disease and assess cardiovascular risk. Cleveland Clinic journal of medicine 2012;79:651-61.

3.   Adragao T, Pires A, Branco P, et al. Ankle--brachial index, vascular calcifications and mortality in dialysis patients. Nephrology, dialysis, transplantation : official publication of the European Dialysis and Transplant Association - European Renal Association 2012;27:318-25.

4.   Potier L, Abi Khalil C, Mohammedi K, Roussel R. Use and utility of ankle brachial index in patients with diabetes. European journal of vascular and endovascular surgery : the official journal of the European Society for Vascular Surgery 2011;41:110-6.

5.   Duet M, Virally M, Bailliart O, et al. Whole-body (201)Tl scintigraphy can detect exercise lower limb perfusion abnormalities in asymptomatic diabetic patients with normal Doppler pressure indices. Nuclear medicine communications 2001;22:949-54.

6.   Hoyer C, Sandermann J, Petersen LJ. The toe-brachial index in the diagnosis of peripheral arterial disease. Journal of vascular surgery 2013;58:231-8.

7.   Norgren L, Hiatt WR, Dormandy JA, et al. Inter-society consensus for the management of peripheral arterial disease. International angiology : a journal of the International Union of Angiology 2007;26:81-157.

8.   Rooke TW, Hirsch AT, Misra S, et al. 2011 ACCF/AHA Focused Update of the Guideline for the Management of Patients With Peripheral Artery Disease (updating the 2005 guideline): a report of the American College of Cardiology Foundation/American Heart Association Task Force on Practice Guidelines. Journal of the American College of Cardiology 2011;58:2020-45.

9.   Stacy MR, Zhou W, Sinusas AJ. Radiotracer imaging of peripheral vascular disease. Journal of nuclear medicine : official publication, Society of Nuclear Medicine 2013;54:2104-10.

10.   Schaper NC, Andros G, Apelqvist J, et al. Diagnosis and treatment of peripheral arterial disease in diabetic patients with a foot ulcer. A progress report of the International Working Group on the Diabetic Foot. Diabetes/metabolism research and reviews 2012;28 Suppl 1:218-24.

11.   Siegel ME, Stewart CA. Thallium-201 peripheral perfusion scans: feasibility of single-dose, single-day, rest and stress study. AJR American journal of roentgenology 1981;136:1179-83.

12.   Kailasnath P, Sinusas AJ. Technetium-99m-labeled myocardial perfusion agents: Are they better than thallium-201? Cardiology in review 2001;9:160-72.

13.   Stacy MR, Maxfield MW, Sinusas AJ. Targeted molecular imaging of angiogenesis in PET and SPECT: a review. The Yale journal of biology and medicine 2012;85:75-86.

14.   Cosson E, Paycha F, Tellier P, et al. Lower-limb vascularization in diabetic patients. Assessment by thallium-201 scanning coupled with exercise myocardial scintigraphy. Diabetes care 2001;24:870-4.

15.   Bajnok L, Kozlovszky B, Varga J, Antalffy J, Olvaszto S, Fulop T, Jr. Technetium-99m sestamibi scintigraphy for the assessment of lower extremity ischaemia in peripheral arterial disease. European journal of nuclear medicine 1994;21:1326-32.

16.   Gollnick PD, Sjodin B, Karlsson J, Jansson E, Saltin B. Human soleus muscle: a comparison of fiber composition and enzyme activities with other leg muscles. Pflugers Archiv : European journal of physiology 1974;348:247-55.

17.   Dobrucki LW, Dione DP, Kalinowski L, et al. Serial noninvasive targeted imaging of peripheral angiogenesis: validation and application of a semiautomated quantitative approach. Journal of nuclear medicine : official publication, Society of Nuclear Medicine 2009;50:1356-63.

18.   Stacy MR, Yu da Y, Maxfield MW, et al. Multimodality imaging approach for serial assessment of regional changes in lower extremity arteriogenesis and tissue perfusion in a porcine model of peripheral arterial disease. Circulation Cardiovascular imaging 2014;7:92-9.

19.   Burt RW, Mullinix FM, Schauwecker DS, Richmond BD. Leg perfusion evaluated by delayed administration of thallium-201. Radiology 1984;151:219-24.

.